Pergamon

Int. J. Solids Structures Vol. 33, No. 9, pp. 1355–1367, 1996

0020-7683/96 $15.00 + .00

0020-7683(95)00097-6

FLUTTER AND DIVERGENCE INSTABILITY OF NONCONSERVATIVE BEAMS AND PLATES

Q. H. ZUO and H. L. SCHREYER
Department of Mechanical Engineering, University of New Mexico, Albuquerque, NM 87131, U.S.A.

(*Received* 7 *June* 1994; *in revised form* 14 *April* 1995)

Abstract—For a conservative system, the only possible instability is of divergence type. For a nonconservative system, however, instability can be of divergence, flutter or both, depending on the amount of nonconservativeness. In this paper, we study the instability of a cantilevered beam and a simply supported plate, subjected to a combination of fixed and follower forces. A nonconservative parameter is introduced to provide all possible combinations of these forces. For the beam, instability changes from divergence to flutter at a critical value of this parameter. For values of the parameter above the critical value, the flutter instability remains as the only instability pattern, in contrast to implications in the literature. For the plate, the instability is governed by flutter for a certain range of the nonconservative parameter, even though divergence instability still exists. The range depends on the geometry (aspect ratio) and material property (Poisson's ratio) of the plate.

INTRODUCTION

Instability, or the loss of stability of equilibrium, is said to occur when a small perturbation can grow with time (Seydel, 1988). In the context of linear instability analysis, it is sufficient to consider only the perturbations which are harmonic in time, since any dynamic disturbance can be decomposed into a series of harmonic functions (modes) through the Fourier expansion. The governing differential equation for the perturbation and the associated boundary conditions make all the modes trivial except those with frequencies that satisfy the characteristic equation. These frequencies are called characteristic frequencies and instability can be equivalently defined as the existence of a pair of purely imaginary or truly complex (nonzero real part) conjugate characteristic frequencies. For conservative systems, the frequencies can only be either real or purely imaginary; therefore, the lowest frequency has to pass through the value of zero as the equilibrium changes from stable to unstable. When the frequency is zero, the governing differential equations and the boundary conditions reduce to those for the classical adjacent equilibrium analysis. This argument is exactly the justification of the adjacent equilibrium theory (also called the Euler method), which states that an equilibrium state is unstable if there is another possible equilibrium configuration in an indefinitely small neighborhood of the one under consideration. For conservative systems, the energy method has also been used to determine the instability point. It has been shown by Pearson (1956) that these two methods are completely equivalent. The phenomenon can be characterized as a divergence instability or a static bifurcation of the equilibrium state.

For nonconservative systems, the frequencies can be either real or complex. Therefore, when instability occurs, the lowest frequency can pass through the origin, as for the conservative systems, or two frequencies can approach each other, coincide, and then become complex conjugate. The latter situation is defined as flutter instability, and the load at which the two frequencies coincide is defined as the flutter load. If the flutter load is exceeded, then the perturbation will oscillate harmonically with the coincident frequency, but the magnitude of the oscillation will grow exponentially with time. The situation where one frequency passes through zero is similar to the one for conservative systems, and the adjacent equilibrium method can still be used, even though the problem is nonconservative. This observation has been pointed out by Herrmann and Bungay (1964) as follows: "The breakdown of the Euler method is not a necessary consequence of the nonconservativeness

of the loading", a situation also noticed by Kounadis (1983). The condition for a nonconservative system to have only the divergence instability has been established by Leipholz (1974a, b), Walker (1973, 1977), Inman (1983), and Inman and Olsen (1988). This subclass of nonconservative systems, which was defined as conservative systems of the second kind by Leipholz, can still be analysed by the adjacent equilibrium method. For two such systems, Ly (1991) obtained the equivalent selfadjoint systems and subsequently performed the instability analysis on the selfadjoint systems instead of the original nonselfadjoint ones. For those nonconservative problems that are not conservative systems of the second kind, however, it is possible to have flutter instability. If a problem is governed by flutter, then the adjacent equilibrium method is inadequate and can yield erroneous results (Pflüger, 1950). It can be analysed correctly only with a dynamic perturbation approach.

Although Nikolai had already discovered the inadequacy of the adjacent equilibrium method and, consequently, had applied the dynamic method to determine the instability load for an elastic bar subjected to a follower torque in 1928–1929 (Bolotin, 1963), his work remained unknown in the west for more than 30 years (Herrmann, 1967). Pflüger (1950) was credited as the first to recognize the inadequacy of the Euler method and Ziegler (1952) was the first to apply the dynamic method to the instability problem of nonconservative systems. Bolotin (1963) devoted a whole book to the various aspects of nonconservative problems in the theory of elastic stability, including the instability of rotating shafts, plates and shells in supersonic flows. Herrmann and coworkers [for example, Herrmann and Jong (1965)] studied the subject extensively, especially the destabilizing effects of the damping of elastic systems subjected to follower forces. For the work before 1967, refer to the review article of Herrmann (1967).

One of the simplest nonconservative problems is the cantilevered beam subjected to an end force consisting of a linear combination of fixed axial and follower (tangent to the end) forces. If the follower part of the force is zero, then the problem is governed by a selfadjoint boundary value problem and, hence, the instability is of the divergence type. Conversely, if the fixed part is zero (Beck's beam), the problem is governed by the flutter. Pflüger (1950) concluded, based on the adjacent equilibrium method, that Beck's beam will never lose stability for any value of the load. Although Ziegler resolved the paradox by applying the dynamic perturbation method to a two-degree-of-freedom model of Beck's beam, the correct instability load of the beam was given by Beck (1952). Herrmann and Bungay (1964) seem to have been the first to study the interrelationship between the amount of nonconservativeness of the problem and the governing type of instability by analysing a two-degree-of-freedom model of the cantilevered beam. A nonconservative parameter was introduced to provide a smooth transition from the fixed loading to the follower loading. Based on simplicity, they claimed it is an "unwarranted" complexity to consider the continuous model. In his extensive book on stability theory, Leipholz (1970) also analysed this problem by using the Galerkin method to find an approximate solution to the continuous model. Because one of the boundary conditions is violated by the trial solution, the calculation is fairly complicated. Leipholz gave only a qualitative plot of instability load versus the nonconservative parameter. The difference between Leipholz's results and those of Herrmann and Bungay is quite noticeable, although a jump in instability loads is present in both cases when instability changes from divergence to flutter.

Here, the governing differential equation for the cantilevered beam is solved exactly to obtain the instability load as a function of the nonconservative parameter which represents a combination of fixed and follower forces such that a value of zero defines a fixed force and a value of one defines a follower force. The instability is of divergence type for the lower range of the parameter. At a certain value of this parameter, the divergence instability ceases to exist and the instability becomes the flutter type. Also, a jump in the instability load appears when the instability changes from divergence to flutter. These features are in qualitative agreement with Herrmann and Bungay. However, the instability never changes back to divergence type as the parameter continues to increase, a result which differs from the conclusion based on the two-degree-of-freedom problem. This conclusion may be important because the two-degree-of-freedom model continues to be used to predict other more complex behavior of nonconservative systems (Kounadis, 1991; Thomsen, 1993). It

is not clear if the instability type changes back to divergence in the stability map of Leipholz, because he limited his discussion to a small range of the nonconservative parameter.

Next, a similar study was performed for a rectangular elastic plate as described by Reissner and Wan (1992). The plate is simply supported on two opposite edges and subjected to a uniform distribution of equal and opposite in-plane normal edge stress resultants. Woinowsky-Krieger (1951) gave the divergence instability (or static buckling) load for the plate if the load remains parallel to the plane of the undeformed plate. He claimed that there is no divergence instability for this plate if the load is of follower type (tangent to the deforming edges of the plate). In their short note, Reissner and Wan clearly disproved the claim by finding the divergent instability loads of the plate subject to a follower force and with various combinations of aspect ratio and Poisson's ratio. However, they did not consider the possibility of flutter instability. Therefore, several questions remain unanswered. Is it possible to have flutter instability for the plate under a follower force? If so, is the load at which flutter instability occurs smaller than the one for divergence instability? What is the stability pattern for the plate if the load is of neither purely fixed nor purely follower type, i.e. what is the relationship between the instability pattern and the amount of nonconservativeness?

In this paper, we answer these questions by studying both the divergence and the flutter instability of the loaded plate using dynamic perturbation. By setting the frequency equal to zero, we recover the results of Woinowsky-Krieger (1951), and Reissner and Wan (1992) for a fixed load and for a purely follower load, respectively. In addition, both the divergence and the flutter instability loads for the plate are found for all possible combinations of fixed and follower forces. The result is that the instability is governed by flutter over a range of the nonconservative parameter and the range depends on aspect ratio and Poisson's ratio. Since the instabilities for all the plates studied here are governed by divergence when the loading is purely follower ($\eta = 1$), the static buckling loads given by Reissner and Wan can be safely used as the instability load for this loading case.

MATHEMATICAL FORMULATIONS

Cantilevered beams

Consider a beam fixed at one end and loaded axially at the other by a force P. If E denotes Young's modulus, I the second area moment, ρ the mass density and A the cross-sectional area, then the equation of motion for the lateral displacement y in a perturbed state is

$$y^{iv} + \alpha^2 y'' + \rho^* \ddot{y} = 0, \tag{1}$$

where

$$\alpha^2 = \frac{P}{EI} \quad \rho^* = \frac{\rho A}{EI}.$$

Primes and dots denote derivatives with respect to the spatial variable, x, and the temporal variable, t, respectively. The fixed end is taken to be $x = 0$ so that $y(0, t) = 0$ and $y'(0, t) = 0$. The zero moment condition at the other end, $x = L$, is $y''(L, t) = 0$. For the loading condition, suppose a linear combination of axial and follower loads is considered (Fig. 1)

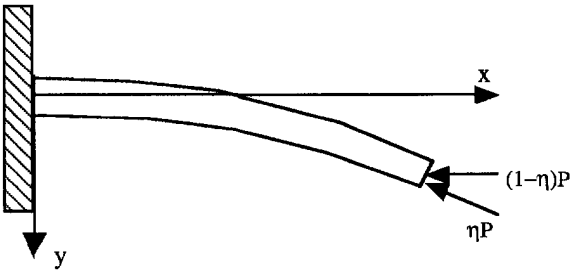

Fig. 1. Linear combination of axial and follower forces on a cantilevered beam.

where the parameter, η, is used to denote the combination such that $\eta = 0$ describes the axial case and $\eta = 1$ the follower case. Note that, under small deformation, the loading is equivalent to that used by Herrmann and Bungay, and Leipholz. Only $\eta = 0$ provides a conservative (selfadjoint) loading case. The result is that the remaining boundary condition becomes

$$y'''(L,t)+(1-\eta)\alpha^2 y'(L,t) = 0. \tag{2}$$

A separation of variables solution $y(x,t) = Y(x)T(t)$ for eqn (1) yields

$$\frac{\ddot{T}}{T} = -\frac{Y^{iv}+\alpha^2 Y''}{\rho^* Y} = -\omega^2. \tag{3}$$

A spatial solution of the type $Y(x) = \exp(\lambda x)$ yields the following equation:

$$\lambda^4+\alpha^2\lambda^2-\rho^*\omega^2 = 0. \tag{4}$$

With

$$\lambda_1 = \sqrt{\tfrac{1}{2}(-\alpha^2+\sqrt{\alpha^4+4\rho^*\omega^2})}$$
$$\lambda_2 = \sqrt{\tfrac{1}{2}(\alpha^2+\sqrt{\alpha^4+4\rho^*\omega^2})}, \tag{5}$$

the spatial part of the solution is

$$Y = A\cosh(\lambda_1 x)+B\sinh(\lambda_1 x)+C\cos(\lambda_2 x)+D\sin(\lambda_2 x). \tag{6}$$

The use of the boundary conditions yields the characteristic equation

$$G(\omega^2,\eta,\alpha^2) \equiv \begin{vmatrix} C_{11} & C_{12} \\ C_{21} & C_{22} \end{vmatrix} = 0, \tag{7}$$

where

$$C_{11} = \lambda_1^2\cosh(\lambda_1 L)+\lambda_2^2\cos(\lambda_2 L)$$
$$C_{12} = \lambda_1^2\sinh(\lambda_1 L)+\lambda_1\lambda_2\sin(\lambda_2 L)$$
$$C_{21} = \lambda_1[\lambda_1^2+(1-\eta)\alpha^2]\sinh(\lambda_1 L)-\lambda_2[\lambda_2^2-(1-\eta)\alpha^2]\sin(\lambda_2 L)$$
$$C_{22} = \lambda_1[\lambda_1^2+(1-\eta)\alpha^2]\cosh(\lambda_1 L)+\lambda_1[\lambda_2^2-(1-\eta)\alpha^2]\cos(\lambda_2 L). \tag{8}$$

For a given loading, i.e. both η and P (or α^2) are specified, the frequencies for the nontrivial perturbation are the solutions of the characteristic equation (7). In general, an analytical expression for ω^2 is not available. However, a simple root-finder like the bisection method works well to obtain the first two frequencies for given η and P.

Since the perturbation involves $\exp(i\omega t)$, the equilibrium is stable if and only if all of the ω^2 values are positive and distinct. The divergence instability load is the smallest value of P for which $\omega^2 = 0$ is a solution of eqn (7). With $\omega^2 = 0$, the characteristic equation (7) reduces to

$$\cos(\alpha L) = \frac{\eta}{\eta-1}, \tag{9}$$

which was given by Panovko and Gubanova (1965). The solution to eqn (9) gives the divergence instability load:

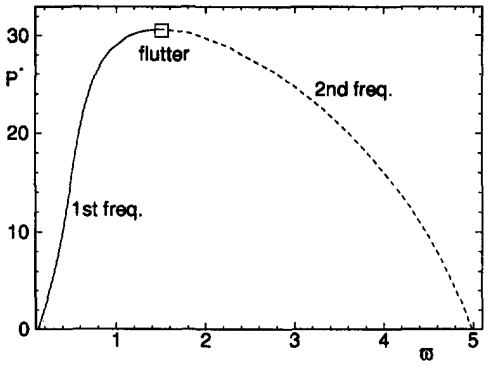

Fig. 2. Non-dimensional load P^* versus nondimensional frequency $\bar{\omega}$ for $\eta = 1.5$.

$$P_i = [\cos^{-1}(\eta/\eta - 1)]^2 EI/L^2. \tag{10}$$

Since a solution to eqn (10) exists only for $\eta \leqslant 0.5$, it is impossible for the beam to have divergence instability for $\eta > 0.5$. This result is different from the conclusion of Herrmann and Bungay based on a two-degree-of-freedom approximation, in which case the instability changes back to divergence type for $\eta > 1$. For $\eta = 0$, the follower part of the load is zero, the instability is of divergence type and the instability load is the classical buckling load, $2.46\ EI/L^2$. Although the problem is conservative only for $\eta = 0$, the divergence instability or static bifurcation exists for $\eta \leqslant 0.5$.

The flutter instability load is the smallest value of P for which the characteristic equation (7) admits a repeated frequency. With a further increase of P beyond the flutter load, the frequencies become complex conjugate and the perturbation will oscillate with a definite frequency but growing amplitude. For $\eta > 0.5$, the only possible instability is of the flutter type. Specifically, for $\eta = 1$, the load is a pure follower one and the characteristic equation becomes

$$(2\rho^*\omega^2 + \alpha^4) + 2\rho^*\omega^2 \cosh(\lambda_1 L)\cos(\lambda_2 L) + \alpha^2\sqrt{\rho^*\omega^2}\sinh(\lambda_1 L)\sin(\lambda_2 L) = 0, \tag{11}$$

which was given by Timoshenko and Gere (1961). The corresponding flutter load is $P_f = 20.05\ EI/L^2$, about eight times the instability load for $\eta = 0$.

For $0 \leqslant \eta \leqslant 1$, the load versus frequency curves have the same features as those in Herrmann and Bungay; therefore, they are not presented here. Figure 2 shows the nondimensional load P^* ($P^* = PL^2/EI$) versus the first two nondimensional frequencies ($\bar{\omega} = \omega^2 L^4 \rho^*/\pi^4$) for $\eta = 1.5$. When $P = 0$, the first two natural frequencies of the beam $\bar{\omega}_1 = 0.127$ and $\bar{\omega}_2 = 5.0$ (values of 0.125 and 4.86, respectively, by Timoshenko and Gere) are obtained. As P increases, the first frequency increases monotonically, while the second one decreases. At $P^* = 30.63$, two frequencies coincide. Any further increase of P will yield two complex conjugate frequencies. Therefore, the flutter load is $P_f = 30.63\ EI/L^2$. The plot shows there is no divergence instability for $\eta = 1.5$. This plot is typical for all values of η larger than 0.5.

The instability (divergence or flutter) load, P_i^* has been obtained for all values of η. A plot of P_i^* as a function of η is shown in Fig. 3. The load increases smoothly from the classical value at $\eta = 0$ except for the jump that appears at $\eta = 0.5$, where the transition from divergence to flutter takes place. The corresponding transition value given by Herrmann and Bungay is $\eta = 5/9$. The key difference is that the instability is of flutter type for $\eta > 0.5$, instead of for $5/9 < \eta < 1.3$, which is the range predicted by the two-degree-of-freedom model. For $\eta > 10$, the flutter load is close to the asymptotic value of $47.80\ EI/L^2$ which holds for large η.

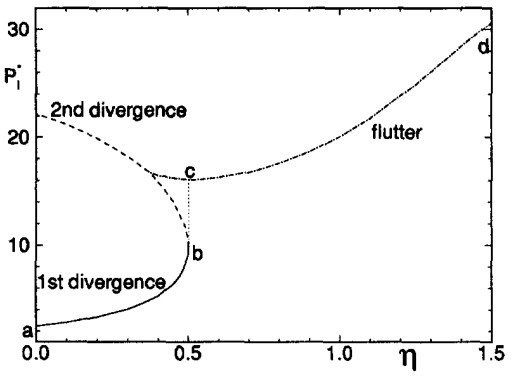

Fig. 3. Instability load parameter P_1^*versus η for the cantilevered beam.

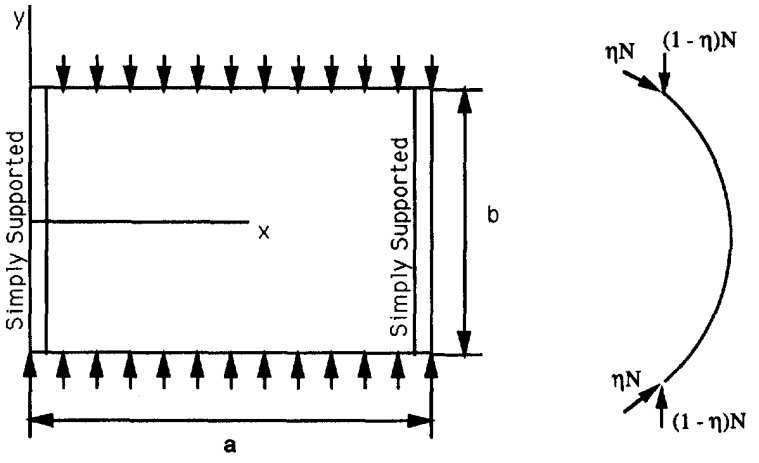

Fig. 4. A simply supported plate subject to axial and follower forces.

Simply supported plate

Consider the instability of the elastic thin plate studied by Reissner and Wan (1992). The plate is simply supported on two opposite edges and subjected to a uniform distribution of equal and opposite in-plane normal edge stress resultants, as shown in Fig. 4. The nonconservative parameter, η, is defined completely analogously to that for the cantilevered beam. The load they considered is either conservative (i.e. the load remains parallel to the undeflected middle-plane of the plate), which corresponds to $\eta = 0$, or a purely follower one (the load remains tangential to the deflected middle-plane of the plate), which corresponds to $\eta = 1$. Here, η is allowed to assume values between 0 and 1. In order to consider the possibility of flutter in addition to divergence instability, a dynamic perturbation is initiated for which the lateral deflection, w, is governed by the differential equation:

$$D\nabla^4 w + Nw_{,yy} + \rho h\ddot{w} = 0. \tag{12}$$

The associated boundary conditions are the same as those in Reissner and Wan:

$$x = 0, a: \quad w = 0, \quad D(w_{,xx} + \nu w_{,yy}) = 0 \tag{13}$$

$$y = \pm\frac{b}{2}: \{D(w_{,yy} + \nu w_{,xx}) = 0, \quad D[w_{,yyy} + (2-\nu)w_{,yxx}] + (1-\eta)Nw_{,y}\} = 0, \tag{14}$$

where D, ρ, h are the bending stiffness, density and the thickness of the plate, ν is Poisson's

ratio and N is the uniform thrust acting on the plate. If the perturbation w is of the form of $\sin(\pi x/a)f(\pi y/a)\exp(i\omega t)$, then eqn (13) is satisfied automatically and f must satisfy

$$f^{iv}-(2-k)f''+(1-\alpha)f=0. \tag{15}$$

In eqn (15), $f'=df/d\xi=a/\pi(df/dy)$ with $\xi=\pi y/a$, and the nondimensional load $k=Na^2/\pi^2D$. The nondimensional parameter $\alpha=\rho ha^4\omega^2/D\pi^4$ is also introduced for the flutter analysis. The associated boundary conditions are

$$f''(\pm\lambda)-\nu f(\pm\lambda)=f'''(\pm\lambda)-\sigma f'(\pm\lambda)=0, \tag{16}$$

where $\lambda=(\pi/2)(b/a)$ and $\sigma=2-\nu-(1-\eta)k$.

There are two forms of solutions for f in the divergence instability analysis by Reissner and Wan, depending on whether or not k is larger than 4. f will be of hypertrigonometric type for $k>4$, and trigonometric type for $k<4$. However, for a dynamic perturbation analysis, there are four types of solutions according to a range of values for both α and k.

(i) $\alpha>1$

$$f(\xi)=c_{1o}\sinh(p_1\xi)+c_{2o}\sin(p_2\xi)+c_{1e}\cosh(p_1\xi)+c_{2e}\cos(p_2\xi), \tag{17}$$

where

$$\begin{aligned}p_1&=\sqrt{(1-k/2)+\sqrt{(1-k/2)^2+(\alpha-1)}}\\ p_2&=\sqrt{-(1-k/2)+\sqrt{(1-k/2)^2+(\alpha-1)}}.\end{aligned} \tag{18}$$

The substitution of eqn (17) in eqn (16) yields two characteristic equations relating the load parameter k and the frequency parameter α; one for the even mode,

$$\begin{aligned}G_e(k,\alpha)&=\begin{vmatrix}(p_1^2-\nu)\cosh(p_1\lambda) & -(p_2^2+\nu)\cos(p_2\lambda)\\ p_1(p_1^2-\sigma)\sinh(p_1\lambda) & p_2(p_2^2+\sigma)\sin(p_2\lambda)\end{vmatrix}\\ &=p_2(p_1^2-\nu)(p_2^2+\sigma)\cosh(p_1\lambda)\sin(p_2\lambda)+p_1(p_1^2-\sigma)(p_2^2+\nu)\sinh(p_1\lambda)\cos(p_2\lambda)=0,\end{aligned} \tag{19}$$

and one for the odd mode,

$$\begin{aligned}G_o(k,\alpha)&=p_2(p_1^2-\nu)(p_2^2+\sigma)\sinh(p_1\lambda)\cos(p_2\lambda)\\ &\quad -p_1(p_1^2-\sigma)(p_2^2+\nu)\cosh(p_1\lambda)\sin(p_2\lambda)=0.\end{aligned} \tag{20}$$

(ii) $[1-(1-k/2)^2]<\alpha<1$

The solution type depends on whether or not k is larger than 2. For $0\leqslant k<2$,

$$f(\xi)=c_{1o}\sinh(p_1\xi)+c_{2o}\sinh(p_2\xi)+c_{1e}\cosh(p_1\xi)+c_{2e}\cosh(p_2\xi), \tag{21}$$

where

$$\begin{aligned}p_1&=\sqrt{(1-k/2)+\sqrt{(1-k/2)^2+(\alpha-1)}}\\ p_2&=\sqrt{(1-k/2)-\sqrt{(1-k/2)^2+(\alpha-1)}},\end{aligned} \tag{22}$$

and the corresponding characteristic equations for the even and odd modes are

$$G_e(k,\eta,\alpha) = \begin{vmatrix} (p_1^2-\nu)\cosh(p_1\lambda) & (p_2^2-\nu)\cosh(p_2\lambda) \\ p_1(p_1^2-\sigma)\sinh(p_1\lambda) & p_2(p_2^2-\sigma)\sinh(p_2\lambda) \end{vmatrix} = 0 \tag{23}$$

and

$$G_o(k,\eta,\alpha) = \begin{vmatrix} (p_1^2-\nu)\sinh(p_1\lambda) & (p_2^2-\nu)\sinh(p_2\lambda) \\ p_1(p_1^2-\sigma)\cosh(p_1\lambda) & p_2(p_2^2-\sigma)\cosh(p_2\lambda) \end{vmatrix} = 0. \tag{24}$$

For $k \geqslant 2$,

$$f(\xi) = c_{1o}\sin(p_1\xi) + c_{2o}\sin(p_2\xi) + c_{1e}\cos(p_1\xi) + c_{2e}\cos(p_2\xi), \tag{25}$$

where

$$\begin{aligned} p_1 &= \sqrt{(k/2-1)+\sqrt{(1-k/2)^2+(\alpha-1)}} \\ p_2 &= \sqrt{(k/2-1)-\sqrt{(1-k/2)^2+(\alpha-1)}}, \end{aligned} \tag{26}$$

and the corresponding characteristic equations are

$$G_e(k,\eta,\alpha) = \begin{vmatrix} (p_1^2+\nu)\cos(p_1\lambda) & (p_2^2+\nu)\cos(p_2\lambda) \\ p_1(p_1^2+\sigma)\sin(p_1\lambda) & p_2(p_2^2+\sigma)\sin(p_2\lambda) \end{vmatrix} = 0 \tag{27}$$

and

$$G_o(k,\eta,\alpha) = \begin{vmatrix} (p_1^2+\nu)\sin(p_1\lambda) & (p_2^2+\nu)\sin(p_2\lambda) \\ p_1(p_1^2+\sigma)\cos(p_1\lambda) & p_2(p_2^2+\sigma)\cos(p_2\lambda) \end{vmatrix} = 0. \tag{28}$$

(iii) $\alpha < [1-(1-k/2)^2]$

$$f(\xi) = c_o\sinh(p\xi) + \bar{c}_o\sin(\bar{p}\xi) + c_e\cosh(p\xi) + \bar{c}_e\cosh(\bar{p}\xi), \tag{29}$$

where an overbar denotes the complex conjugate and p^2 is complex:

$$p^2 = (1-k/2) + \mathrm{i}\sqrt{1-(1-k/2)^2-\alpha}. \tag{30}$$

The corresponding characteristic equations are

$$G_e(k,\eta,\alpha) = \begin{vmatrix} (p^2-\nu)\cosh(p\lambda) & (\bar{p}^2-\nu)\cosh(\bar{p}\lambda) \\ p(p^2-\sigma)\sinh(p\lambda) & \bar{p}(\bar{p}^2-\sigma)\sinh(\bar{p}\lambda) \end{vmatrix} = 0 \tag{31}$$

and

$$G_o(k,\eta,\alpha) = \begin{vmatrix} (p^2-\nu)\sinh(p\lambda) & (\bar{p}^2-\nu)\sinh(\bar{p}\lambda) \\ p(p^2-\sigma)\cosh(p\lambda) & \bar{p}(\bar{p}^2-\sigma)\cosh(\bar{p}\lambda) \end{vmatrix} = 0. \tag{32}$$

For a given loading, i.e. if both η and k are specified, the frequencies for the nontrivial perturbation are the solutions of one set (both even and odd modes) of the characteristic equations, depending on the value of k. For a given value of k, a set of values for α (or ω^2) are chosen starting from zero. For each chosen α, a check is made to determine which characteristic function should be used. Care has to been taken when a solution lies in the boundary between two cases. For example, $\alpha = 1 (\text{or } \omega = 9.869\sqrt{D/\rho h a^4})$ is the lowest natural frequency of plates with any value of b/a but zero Poisson's ratio ν (Blevins, 1979). Since $\alpha = 1$ lies on the boundary between cases (i) and (ii), the degenerated form of either eqns (17) or (21) has to be used to find the frequency.

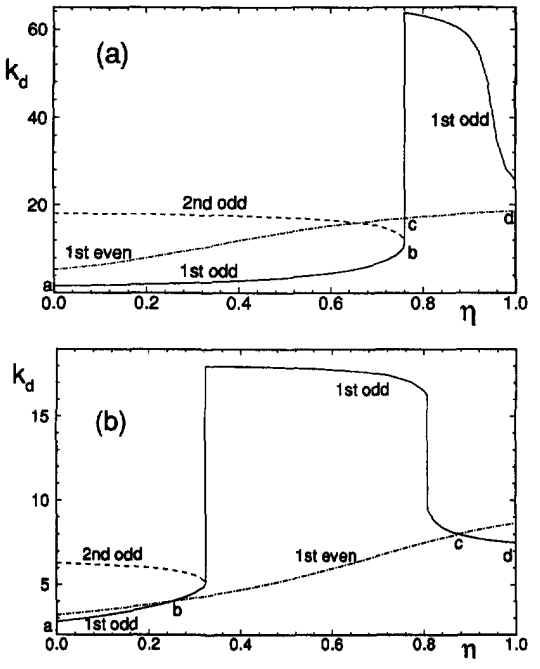

Fig. 5. Divergence instability load k_d versus η for a plate. (a) $b/a = 0.5$, $\nu = 0.3$; (b) $b/a = 1.0$, $\nu = 0.0$.

Since the perturbation involves exp ($i\omega t$), the equilibrium is stable if, and only if, all of the ω^2 values are positive and distinct. Divergence instability loads are the values of P for which $\omega^2 = 0$. Then the solution can only take the form of eqns (25) or (29) depending on whether or not k is larger than 4. The corresponding characteristic equations (27), (28) and (31), (32) reduce to those in Reissner and Wan, where the divergence loads for $\eta = 0$ (conservative loading) and $\eta = 1$ (follower loading) have been given. They find that the divergence load varies continuously with aspect ratio b/a and Poisson's ratio ν. To supplement their results, we study the dependency of the divergence load on the nonconservative parameter η. Surprisingly, a jump in the load is found for certain combinations of b/a and ν. Figure 5(a) shows the divergence instability load parameter, k_d, versus η for $b/a = 0.5$, and $\nu = 0.3$. For $\eta < 0.76$, the divergence instability is governed by the odd mode and the load increases smoothly with an increase of η. At $\eta = 0.76$, the first two odd divergence loads coincide. Then the divergence load for the odd mode suffers a huge jump. The divergence load for the even mode increases smoothly from $\eta = 0$ to $\eta = 1$ and is lower than that for the odd mode for $0.76 < \eta \leqslant 1.0$. Therefore, the divergence instability (or static buckling) of the plate is governed by the curve a–b–c–d and the divergence load jumps when the governing mode changes from odd to even.

Although, as indicated by Reissner and Wan, the divergence instability load for $\eta = 1$ is larger than that for $\eta = 0$, the load does not necessarily increase monotonically with η, as one might expect. As shown in Fig. 5(b) for a plate with $b/a = 1$, $\nu = 0$, the divergence load, described by the curve a–b–c–d, changes continuously and reaches a maximum at $\eta = 0.87$.

A nonconservative system has the possibility of flutter in addition to divergence instability. A thorough instability analysis of such a system requires plots of load versus frequency to identify the nature of the instability, to show the key points concerning change in modes, to illustrate jumps in instability loads, and to determine which type of instability actually governs. Plots of the load parameter, k, as a function of nondimensional frequency $\omega^*(\omega^* = \omega\sqrt{\rho h a^4/D})$ for the plate with $b/a = 1$, $\nu = 0.5$ and various values of η are shown in Fig. 6. Figure 6(a) gives results for $\eta = 0$. At $k = 0$, the three lowest natural frequencies of the plate, $\omega_1^* = 9.12$ [9.08 by Blevins (1979)], $\omega_2^* = 14.37, \omega_3^* = 34.78$, are obtained. As k increases, both the odd and even frequencies approach zero monotonically. Although the

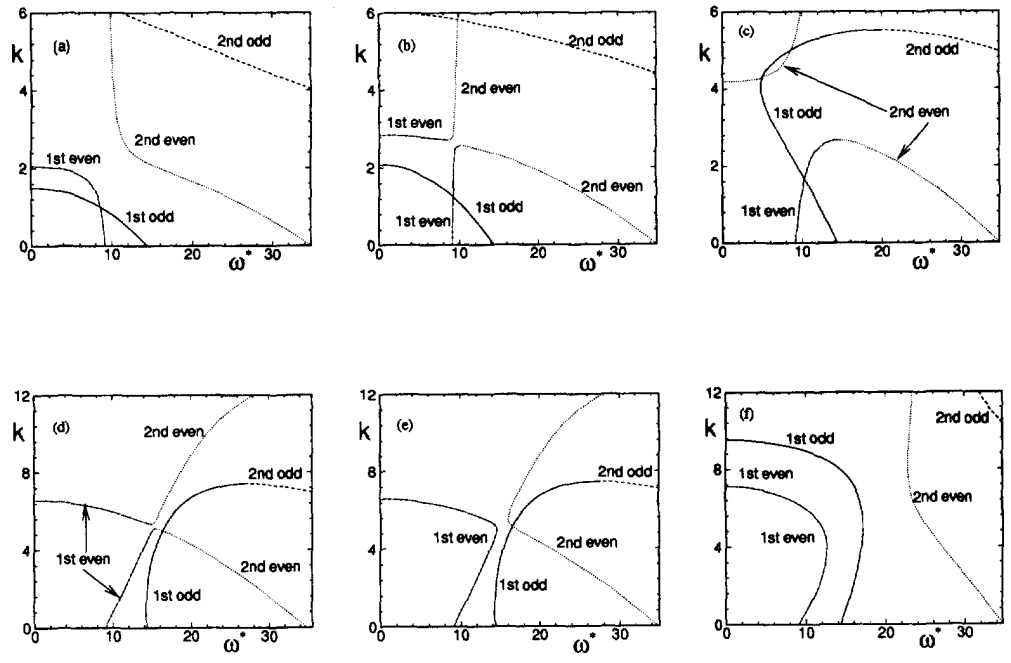

Fig. 6. Load k versus nondimensional frequency ω^* for $b/a = 1$ and $\nu = 0.5$. (a) $\eta = 0$; (b) $\eta = 0.195$; (c) $\eta = 0.4$; (d) $\eta = 0.8$; (e) $\eta = 0.805$; (f) $\eta = 1.0$.

first even frequency starts with a smaller value than the first odd one, the first odd frequency approaches zero at a much faster rate than the even one. The result is that the instability is governed by an odd divergence mode and the instability load parameter is $k_d = 1.5$. As expected, there is no flutter since this is a conservative problem. It is also to be noted that although the first odd and even frequencies coincide at $k = 1.0$, no flutter occurs because a further increase of k beyond 1.0 still provides all real frequencies.

Figure 6(b) shows the load–frequency relationship for $\eta = 0.195$. Although the first odd frequency curve is qualitatively the same as that for $\eta = 0$, the first two even frequency curves are significantly different from those shown in Fig. 6(a). The key difference is that instead of monotonically approaching zero, the first even frequency starts to increase very slowly and eventually coincides with the monotonically decreasing second even frequency at $k = 2.57$. A small increase of k beyond the value of 2.57 makes the frequencies complex conjugates, i.e. flutter occurs at $k_f = 2.57$. Since those two even frequencies reassume real values for $k \geqslant 2.72$, the flutter instability occurs for $2.57 < k < 2.72$. Although a flutter load exists, the plate is still governed by divergence instability since the divergence load associated with odd mode, $k_d = 2.08$, is lower than k_f.

Figure 6(c) shows the load versus frequency for $\eta = 0.4$. The first odd frequency decreases at first, but instead of approaching zero, the curve turns back and meets the second odd frequency, which results in an odd mode flutter instability at $k = 5.52$. The two even frequencies are similar to those shown in Fig. 6(b), and the flutter load parameter is $k_f = 2.68$. Since the divergence load, $k_d = 4.19$, is substantially higher than k_f, this particular plate is governed by flutter, which makes the divergence analysis for the plate unsafe.

Figure 6(d) shows the case for $\eta = 0.8$, where the plate is still governed by flutter, but the range of flutter is very small (from $k = 5.12$ to $k = 5.34$). A small increase of η will make the flutter part disappear, as shown in Fig. 6(e), in which $\eta = 0.805$ and the first two even frequencies are continuous functions of the load parameter, k. The odd mode flutter occurs at $k_f = 7.42$. Since k_f is higher than the divergence load k_d, the instability for this plate is governed by even mode divergence and the load is $k_d = 6.6$.

Finally, results are given in Fig. 6(f) for $\eta = 1$, which is the pure-follower-force problem considered by Reissner and Wan. The curve for the first odd frequency curls back to the k axis again, so that a divergence load exists for the odd mode at $k = 9.52$. The two even frequencies are separated much further and the first even frequency approaches zero,

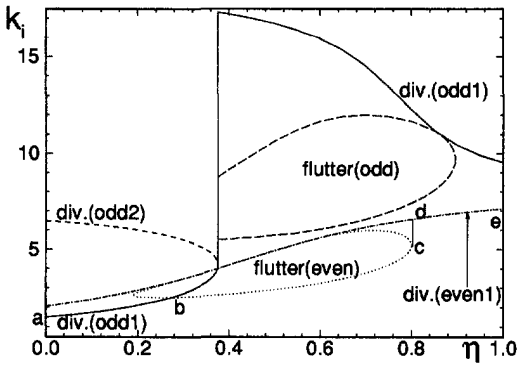

Fig. 7. Instability load k_i versus η for $b/a = 1$ and $\nu = 0.5$.

resulting in an even mode divergence instability at $k = 7.12$. This plot confirms that the results of Reissner and Wan are indeed the instability load for this case.

Figure 7 summarizes the features illustrated in Fig. 6 by giving the instability load parameter, k_i, as a function of η for $b/a = 1$ and $\nu = 0.5$. The pattern of the variation of the divergence instability loads with η is similar to that already discussed in connection with Fig. 5. However, here flutter loads appear. Flutter associated with even modes first appears at $\eta = 0.195$. The region between the lower and upper branches, labeled "flutter (even)," denotes the range of k for given η where flutter associated with even modes can occur. A significant part of the upper branch apparently coincides with the divergence load associated with the first even mode. This "flutter (even)" region terminates at $\eta = 0.8$, after which the plate is again governed by divergence. Similarly, flutter associated with odd modes first exists for k between the lower and upper branches, labeled "flutter (odd)". The upper branch to the left of the intersection with the first odd divergence load corresponds to the coincident frequencies of imaginary values. The "flutter (odd)" region exists over the range $0.38 < \eta < 0.9$, but these flutter loads are higher than the first even divergence load. The instability load of the plate follows the curve described by a–b–c–d–e. The instability of the plate is governed by flutter for $0.27 < \eta < 0.8$; otherwise the plate is governed by divergence. The instability load jumps from "c" to "d" when the governing instability changes back from flutter to divergence. When the plate is governed by flutter, the flutter load can be substantially lower than the divergence load, which makes the divergence buckling analysis using the Euler method unsafe. In Figs 6 and 7, the value of $\nu = 0.5$ is not crucial. Similar results have also been obtained for $\nu = 0.45$.

In general, the range of η over which the plate is governed by flutter depends on both b/a and ν. Figure 8 gives the dependence of the range of the flutter instability on Poisson's ratio for $b/a = 0.5$ and $b/a = 1.0$.

CONCLUSIONS

Previous results for the beam have generally been based on finite-degree-of-freedom models. Although essential features had been illustrated, our analysis shows that incorrect conclusions concerning the type of instability had been made. In the case of plates, solutions exist only for divergence analysis and under a particular form of nonconservative loading. Here, a rather complete solution for both divergence and flutter instability has been given for various nonconservative loadings. Even for this simple plate problem, the analysis yielded an unbelievably complex set of circumstances, involving nonmonotonic and even discontinuous relationships between the instability loads and the parameter describing the degree of nonconservativeness. These results were not previously available and could not have been anticipated based on the existing literature.

The instability of a cantilevered beam and a simply supported plate was studied with the use of dynamic perturbations. For the beam, instead of the two-degree-of-freedom model or a Galerkin approximation to the continuous model, the governing partial differential equation and associated boundary conditions of the continuous model are solved

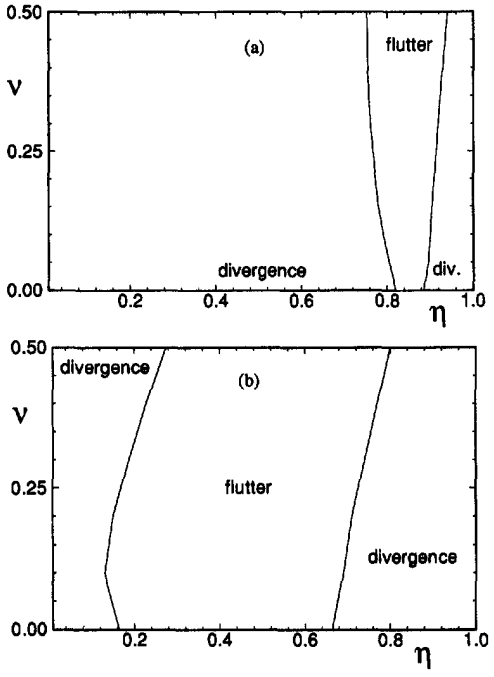

Fig. 8. The range of η over which flutter governs as a function of Poisson's ratio. (a) $b/a = 0.5$; (b) $b/a = 1.0$.

exactly. In addition to more accurate results, it is shown that the instability is governed by flutter for all values of the nonconservative parameter greater than a fixed value.

For the given plate subject to a uniformly distributed nonconservative thrust, both divergent instability and flutter instability loads have been found for all values of the nonconservative parameter, η, between 0 and 1. The divergence instability (or static buckling) load does not depend continuously on η as it does on aspect ratio and Poisson's ratio. Although the instability load for $\eta = 1$ (follower loading) is always larger than that for $\eta = 0$ (conservative loading), the load does not increase monotonically with η. If flutter instability is considered, then there is a particular range of η over which instability of the plate is governed by flutter, although a divergence instability load also exists. The range depends on both the geometric (aspect ratio) and material (Poisson's ratio) parameters. Over the range which flutter governs, the flutter load can be substantially lower than the divergence load, which makes the static buckling analysis of the plate unsafe.

The nonconservative plate problem displays a rich variety of scenarios. Divergence instability can exist for all values of the nonconservative parameter, jumps in the instability loads can exist even for purely divergence cases, switches in the instability pattern can occur with possible jumps in the loads between divergence and flutter, and nonmonotonic variations in instability loads with respect to the nonconservative parameter are possible. It is reasonable to assume that the situation is even more varied for more complex structures. The only safe conclusion that can be deduced from this work is that extreme care must be taken in analysing nonconservative systems that are not conservative systems of the second kind. The existence of a divergence instability is not a sufficient condition that the corresponding instability load governs. Instead, the fundamental approach associated with load–frequency plots based on dynamic perturbations must be followed to ensure that the true instability load is obtained.

Acknowledgement—This research was supported in part by grant no. MSS 9203747 from the National Science Foundation to the University of New Mexico.

REFERENCES

Beck, M. (1952). Die Knicklast des einseitig eingespannten, tangential gedrückten Stabes. *Z. Angew. Math. Phys.* **3,** 225–228.

Blevins, R. D. (1979). *Formulas for Natural Frequency and Mode Shape*. Von Nostrand Reinhold, New York.

Bolotin, V. V. (1963). *Nonconservative Problems of the Theory of Elastic Stability* (English translation, edited by G. Herrmann). Pergamon Press, Oxford.

Herrmann, G. (1967). Stability of equilibrium of elastic systems subjected to nonconservative forces. *Appl. Mech. Rev.* **20,** 103–108.

Herrmann, G. and Bungay, R. W. (1964). On the stability of elastic systems subjected to nonconservative forces. *J. Appl. Mech.* **31,** 435–440.

Herrmann, G. and Jong, I.-C. (1965). On the destabilizing effect of damping in nonconservative elastic systems. *J. Appl. Mech.* **32,** 592–597.

Inman, D. J. (1983). Dynamics of asymmetric nonconservative systems. *J. Appl. Mech.* **50,** 199–203.

Inman, D. J. and Olsen, C. L. (1988). Dynamics of symmetrizable nonconservative systems. *J. Appl. Mech.* **55,** 206–212.

Kounadis, A. N. (1983). The existence of regions of divergence instability for nonconservative systems under follower forces. *Int. J. Solids Structures* **19,** 725–733.

Kounadis, A. N. (1991). Some new instability aspects for nonconservative systems under follower loads. *Int. J. Mech. Sci.* **33,** 297–331.

Leipholz, H. H. E. (1974a). On conservative elastic systems of the first and second kind. *Ing. Arch.* **43,** 255–271.

Leipholz, H. H. E. (1974b). On a generalization of the self-adjointness and of Rayleigh's quotient. *Mech. Res. Commun.* **1,** 67–72.

Leipholz, H. H. E. (1970). *Stability Theory, An Introduction to the Stability of Dynamic Systems and Rigid Bodies* (Translated from *Stabilitätstheorie*, published in 1968). Academic Press, New York.

Ly, B. L. (1991). Symmetrization of some conservative systems of the second kind. *J. Appl. Mech.* **58,** 1098–1101.

Panovko, Y. G. and Gubanova, I. I. (1965). *Stability and Oscillations of Elastic Systems, Paradoxes, Fallacies, and New Concepts*. Consultants Bureau Enterprises, New York.

Pearson, C. E. (1956). General theory of elastic stability. *Q. Appl. Math.* **14,** 133–144.

Pflüger, A. (1950). *Stabilitätsprobleme der Elastostatik*. Springer, Berlin.

Reissner, E. and Wan, F. Y. M. (1992). A follower load buckling problem for rectangular plates. *J. Appl. Mech.* **59,** 674–676.

Seydel, R. (1988). *From Equilibrium To Chaos*. Elsevier Science, New York.

Thomsen, J. J. (1993). Chaotic dynamics of the partially follower-loader elastic double-pendulum. The Danish Center for Applied Mathematics and Mechanics, Report no. 455.

Timoshenko, S. P. and Gere, J. M. (1961). *Theory of Elastic Stability*, 2nd Edn. McGraw-Hill, New York.

Walker, J. A. (1973). Energy-like Liapunov functions for linear elastic systems on a Hilbert space. *Q. Appl. Math.* **30,** 465–480.

Walker, J. A. (1977). Liapunov analysis of the generalized pflüger problem. *J. Appl. Mech.* **39,** 935–938.

Woinowsky-Krieger, S. (1951). Uber die Beulsicherheit von Rechteckplatten mit quervershieblichen Rändern. *Ing. Arch.* **19,** 200–207.

Ziegler, H. (1952). Die Stabilitätskriterien der elastomechanik. *Ing. Arch.* **20,** 49–56.